

Copyright © 2003, Paper 7-012; 5,129 words, 5 Figures, 0 Animations, 1 Table.  
<http://EarthInteractions.org>

# Variability in Terrestrial Carbon Sinks over Two Decades. Part I: North America

**C. Potter\***

NASA Ames Research Center, Moffett Field, California

**S. Klooster**

California State University, Monterey Bay, Seaside, California

**P. Tan, M. Steinbach, V. Kumar**

University of Minnesota, Minneapolis, Minnesota

**V. Genovese**

California State University, Monterey Bay, Seaside, California

Received 29 May 2003; accepted 7 July 2003

**ABSTRACT:** Seventeen years (1982–98) of net carbon flux predictions from a simulation model based on satellite observations of monthly vegetation cover have been analyzed. The NASA–CASA model was driven by vegetation cover properties derived from the Advanced Very High Resolution Radiometer and radiative transfer algorithms that were developed for the Moderate Resolution Imaging Spectroradiometer (MODIS). It is found that although the terrestrial ecosystem sink for atmospheric CO<sub>2</sub> on the North American continent has been fairly consistent at between +0.2 and +0.3 Pg C yr<sup>-1</sup>, high

---

\* Corresponding author address: C. Potter, NASA Ames Research Center, Moffett Field, CA 94035.

E-mail address: [cpotter@mail.arc.nasa.gov](mailto:cpotter@mail.arc.nasa.gov)

interannual variability in net ecosystem production (NEP) fluxes can be readily identified at locations across the continent. Five major areas having the highest variability were detected: 1) along the extreme northern vegetated zones of Canada and Alaska, 2) the northern Rocky Mountains, 3) the central-western U.S. Great Plains and central farming region, 4) across the southern United States and Mexico, and 5) in coastal forest areas of the United States and Canada. Analysis of climate anomalies over this 17-yr time period suggests that variability in precipitation and surface solar irradiance could be associated with trends in carbon sink fluxes within regions of high NEP variability.

**KEYWORDS:** Carbon cycle, Remote sensing, Model

## 1. Introduction

Carbon sequestration in ecosystems involves the net uptake of CO<sub>2</sub> from the atmosphere for persistent storage in sinks of terrestrial vegetation or soil pools. Land areas that consistently sequester carbon by growth in net ecosystem production are potentially important as future sinks for industrial CO<sub>2</sub> emissions. Conversely, land areas that do not consistently sequester carbon over time may be adding to already increasing atmospheric CO<sub>2</sub> from fossil fuel-burning sources.

Efforts are under way in the United States and elsewhere to develop systems of carbon “credit trading,” in which, for instance, industrial emitters of CO<sub>2</sub> may pay other entities, such as the owners of reforested land, for enhancements that result in net carbon sequestration to help mitigate the impacts of the industrial greenhouse gas emissions. Therefore, accurate estimates of how much carbon various ecosystems can absorb, and how variable large-scale carbon sink or source fluxes are from year to year, will be fundamental to a successful system of carbon credit trading.

As a first approximation, lumped box models can be used to study biosphere-atmosphere exchange rates for trace gases, without regard for terrestrial vegetation types, ecological limitations, or interannual climate effects on CO<sub>2</sub> uptake and storage potential on land (Bolin, 1981). Although one can use a simple box model for order of magnitude estimates of carbon fluxes, these formulations are not sufficient for determining the spatial and temporal variability of a terrestrial carbon sink. Another modeling approach is to discretize the terrestrial biosphere into thousands of georeferenced pixels, with detailed physiological processes simulated for each pixel to transport CO<sub>2</sub> between the simulated land surface and the atmosphere, and to store carbon at the pixel location (e.g., Potter et al., 1993; Maisongrande et al., 1995; Kindermann et al., 1996; McGuire et al., 2001). This spatial modeling approach considers not only actual vegetation types, but also the historical changes in land cover properties and vegetation type at each pixel location using satellite remote sensing. In addition, the effect of simultaneous plant, soil, and climate impacts can be captured in the physiological process description, which is uniquely valuable in a domain where there is still a sparse distribution of long-term field study sites of these effects from which to gather net ecosystem production (NEP) data for continental-scale interpolations.

A computer model of this type based on satellite sensor measurements of vegetation cover has been developed to simulate global ecosystem carbon cycling

(Potter, 1999; Potter et al., 2003a). The National Aeronautics and Space Administration–Carnegie Ames Stanford Approach (NASA–CASA) model is designed to estimate monthly patterns in plant carbon fixation, plant biomass, nutrient allocation, litter fall, soil nutrient mineralization, and carbon emissions from soils worldwide. This results in spatially discrete predictions of NEP over nearly two decades. Direct input of satellite sensor “greenness” data from the Advanced Very High Resolution Radiometer (AVHRR) sensor into the NASA–CASA model are used to estimate spatial variability in monthly net primary production (NPP), biomass accumulation, and litter fall inputs to soil carbon pools at a geographic resolution of  $0.5^\circ$  latitude–longitude. Global NPP of vegetation is predicted using the relationship between greenness reflectance properties and the fraction of absorption of photosynthetically active radiation (FPAR), assuming that net conversion efficiencies of PAR to plant carbon can be approximated for different ecosystems or are nearly constant across all ecosystems (Nemani and Running, 1989; Sellers et al., 1994; Goetz and Prince, 1998; Running and Nemani, 1998).

In this study, we analyze the NEP results of NASA–CASA model predictions from 1982 to 1998 to infer variability in subcontinental-scale carbon fluxes and to better understand climate control patterns over terrestrial carbon sinks. The similar CASA NPP model application by Hicke et al. (Hicke et al., 2002) to North America began to address a subset of these issues. The scope of our study goes well beyond those of previous CASA applications, however, in that we present here the first of a three-part global biosphere analysis of variability in  $\text{CO}_2$  sinks, starting with North America, and subsequently extending the analysis to Eurasia, South America, Africa, and Australia. Moving beyond the approach of Hicke et al. (Hicke et al., 2002), we report complete NASA–CASA model results for continental NEP (Potter et al., 2003a), including predicted soil  $\text{CO}_2$  respiration fluxes in addition to NPP estimates.

## 2. Global data and models

For this analysis, terrestrial NEP fluxes have been computed monthly (over the period 1982–98) at a spatial resolution of  $0.5^\circ$  latitude–longitude using the NASA–CASA biosphere model (Potter, 1999; Potter et al., 1999; Potter et al., 2003a). NASA–CASA is a numerical model of monthly fluxes of water, carbon, and nitrogen in terrestrial ecosystems (Figure 1). Our estimates of terrestrial NPP fluxes depend on inputs of global satellite observations for land surface properties and on gridded model drivers from interpolated weather station records (New et al., 2000) distributed across all the continental masses.

Our fundamental approach to estimating NPP is to define optimal metabolic rates for carbon fixation processes and to adjust these rate values using factors related to limiting effects of time-varying inputs of solar radiation (SOLAR), air temperature (TEMP), precipitation (PREC; New et al., 2000), predicted soil moisture, and land cover (DeFries and Townshend, 1994). Carbon ( $\text{CO}_2$ ) fixed by vegetation as NPP is estimated in the ecosystem model according to the time-varying (monthly mean) FPAR intercepted by plant canopies and a light utilization efficiency term ( $e_{\text{max}}$ ). This product is modified by stress factors for temperature

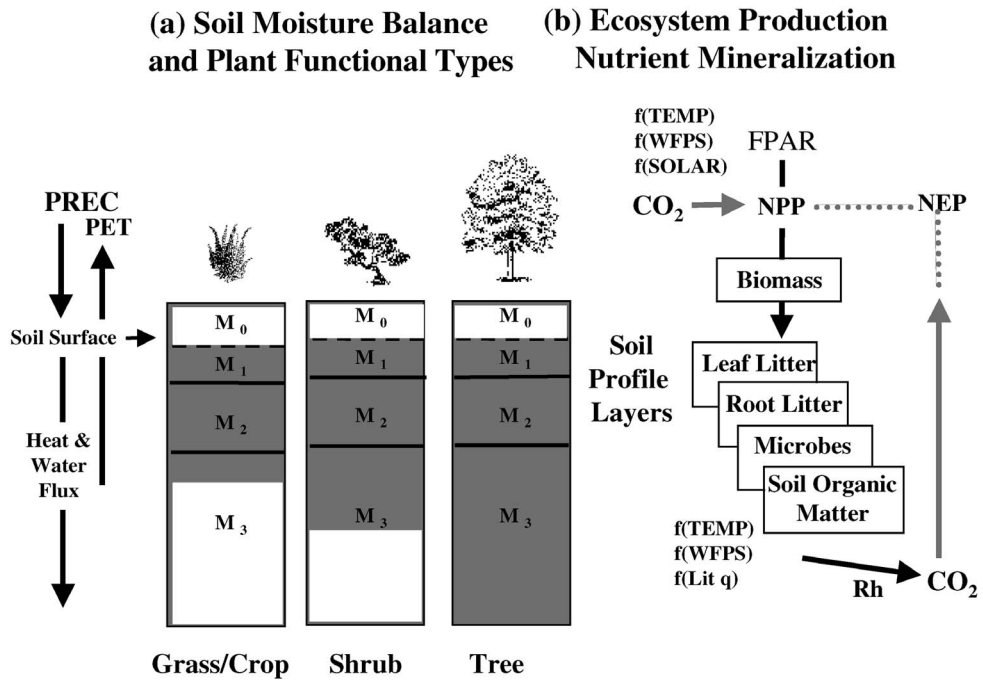


**Figure 1.** Schematic representation of components in the NASA-CASA model. (a) The soil profile component is layered with depth into a surface ponded layer ( $M_0$ ), a surface organic layer ( $M_1$ ), a surface organic-mineral layer ( $M_2$ ), and a subsurface mineral layer ( $M_3$ ), showing typical levels of soil water content (shaded) in three general vegetation types. (b) The production and decomposition component shows separate pools for carbon cycling among pools of leaf litter, root litter, woody detritus, microbes, and soil organic matter. Microbial respiration rate is controlled by soil temperature (TEMP) and litter quality (LIT  $q$ ). WFPS is water-filled pore space in soils.

( $T_a$ ) and moisture ( $W$ ) that vary over time and space. The  $e_{\max}$  term is set uniformly at  $0.39 \text{ g C (MJ}^{-1} \text{ PAR)}$  (Potter et al., 1993), a value that has been verified globally by comparing predicted annual NPP to more than 1900 field estimates of NPP (Potter et al., 2003a). Interannual NPP fluxes from the CASA model have been reported (Behrenfeld et al., 2001) and checked for accuracy by comparison to multiyear estimates of NPP from field stations and tree rings (Malmström et al., 1997) and forest inventory reports (Hicke et al., 2002). Our NASA-CASA model has been validated against field-based measurements of NEP fluxes and carbon pool sizes at multiple locations in North America (Potter et al., 2001; Amthor et al., 2001; Potter et al., 2003a).

Our NASA-CASA model is designed to couple seasonal patterns of NPP to soil heterotrophic respiration ( $R_h$ ) of  $\text{CO}_2$  from soils worldwide (Potter, 1999). First-order decay equations simulate exchanges of decomposing plant residue (metabolic and structural fractions) at the soil surface. The model also simulates surface soil organic matter (SOM) fractions that presumably vary in age and chemical

composition. Turnover of active (microbial biomass and labile substrates), slow (chemically protected), and passive (physically protected) fractions of the SOM are represented.

Global soils data for this version of NASA–CASA come from the most recent Food and Agriculture Organization (FAO, 1995). Predominant soil type and texture have been determined for each  $0.5^\circ$  grid cell in the model simulations. The major scale discrepancies between these FAO soil polygon data and global satellite datasets used to drive NPP will be in remote desert and high-latitude zones, where the abundance of soil survey information is the weakest, and NPP is the lowest. These FAO soil attributes influence storage potential of carbon in the upper 20–30 cm of the simulated soil profile, with deep clay soils storing more organic matter than lighter sandy soils.

NEP is computed as NPP minus total  $R_h$  fluxes, excluding the effects of small-scale fires and other localized disturbances or vegetation regrowth patterns on carbon fluxes (Schimel et al., 2001). The effects of large-scale ( $0.5^\circ$  grid area) disturbances on the continental carbon cycle has been addressed for the NASA–CASA model in Potter et al. (Potter et al., 2003b).

Whereas previous versions of the NASA–CASA model (Potter et al., 1993; Potter et al., 1999) used a normalized difference vegetation index (NDVI) to estimate FPAR, the current model version instead relies upon canopy radiative transfer algorithms (Knyazikhin et al., 1998), which are designed to generate improved spatially varying FPAR products as inputs to carbon flux calculations. These radiative transfer algorithms, developed for the Moderate Resolution Imaging Spectroradiometer (MODIS) aboard the NASA *Terra* platform, account for attenuation of direct and diffuse incident radiation by solving a three-dimensional formulation of the radiative transfer process in vegetation canopies. Monthly gridded composite data from spatially varying channels 1 (visual red) and 2 (near infrared) of the AVHRR have been processed according to the MODIS radiative transfer algorithms and aggregated over the global land surface to  $0.5^\circ$  grid resolution, consistent with the NASA–CASA model driver data for climate variables. To minimize cloud contamination effects, a maximum value composite algorithm was applied spatially for  $0.5^\circ$  pixel values.

### 3. Variability in terrestrial carbon sinks

For global comparison purposes, we define the continental area for North America (NA) as latitude zones higher than  $13.5^\circ\text{N}$  within longitude zones from the Pacific date line to the eastern side of the Atlantic Ocean. In terms of predicted annual NPP, the NA continent was estimated to vary between 6 and  $7.5 \text{ Pg C}$  ( $1 \text{ Pg} = 10^{15} \text{ g}$ )  $\text{yr}^{-1}$  (Potter et al., 2003a). These results for NA regional NPP fluxes are consistent with those reported by Schimel et al. (Schimel et al., 2001) based largely on predictions from numerous other global ecosystem models and inventories. As an example, Hicke et al. (Hicke et al., 2002) likewise estimated annual NPP for NA (north of  $22^\circ\text{N}$ ) at  $6.2 \text{ Pg C yr}^{-1}$ , using higher spatial resolution (8 km) satellite sensor inputs to the CASA vegetation model.

Continental-scale NEP results from our NASA–CASA interannual simulations imply that since 1982, the terrestrial NEP sink for atmospheric  $\text{CO}_2$  in NA has been

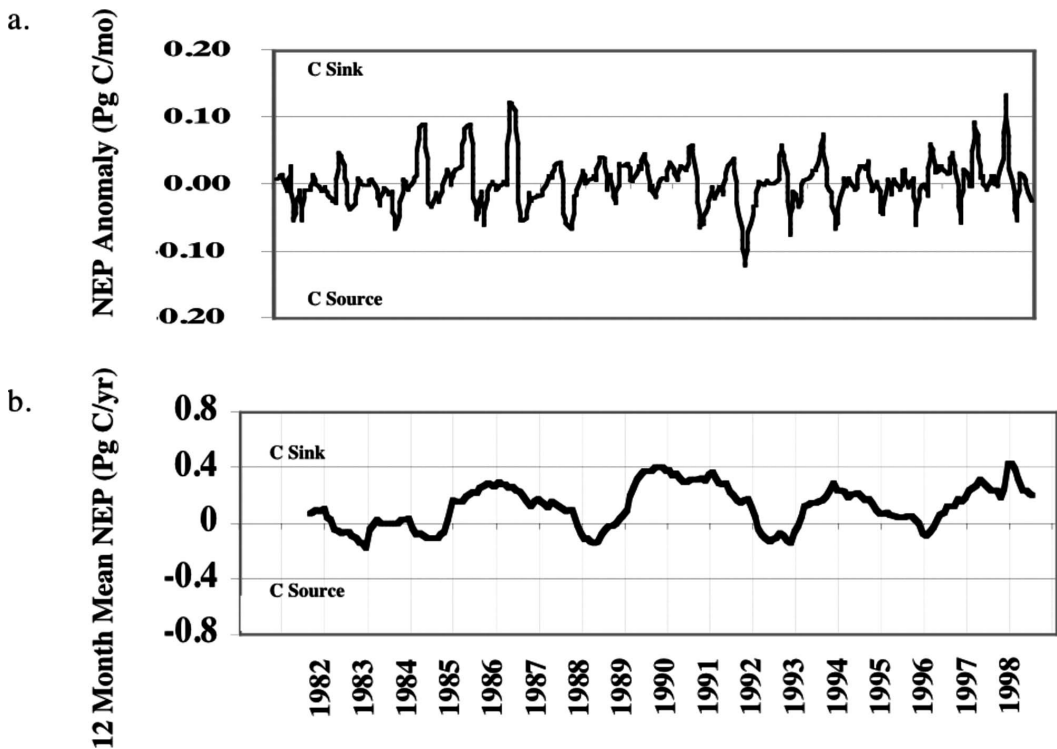


Figure 2. NASA-CASA results from interannual simulations of NEP for NA (a) monthly predictions and (b) 12-month running mean.

fairly consistent at between  $+0.2$  and  $+0.3 \text{ Pg C yr}^{-1}$  (Figure 2; Potter et al., 2003a). The exceptions were during relatively cool yearly periods like 1987, 1991–92, and 1995–96 when the NA continental NEP is predicted to be close to zero net flux of  $\text{CO}_2$ . Although continental NEP sinks may have increased slightly in recent years, the spatial distribution of the NA carbon sink has been quite different from year to year. For example, during 1996, a year not marked by substantial regional warming (cf. 1995) nor by above-average precipitation on a continental scale, the predicted continental sink for carbon is localized mainly along the eastern portions of the United States and southern Canada. In 1997, substantial regional warming and above-average precipitation were observed, leading to a shift in the major sink areas on the continent to northwestern Canada and portions of the central United States. In 1998, a year closely matching 1997 in a total NEP flux of about  $+0.2 \text{ Pg C}$  for NA, regional warming continued and above-average precipitation was observed, leading to another shift in the major sink areas on the continent to southeastern portions of Canada and the United States. Our results are largely consistent with those of Nemani et al. (Nemani et al., 2002), who predicted that the U.S. terrestrial C sink is becoming stronger at least partially in response to increasing precipitation and humidity.

It should be noted that the NASA-CASA model does not explicitly estimate sources of terrestrial carbon emitted to the atmosphere from small-scale ecosystem disturbances, such as from wild fires source fluxes of  $\text{CO}_2$ , nor from other major

land use changes over decades. Nevertheless, we have demonstrated that the FPAR time series can capture sources of terrestrial carbon emitted to the atmosphere from large-scale ecosystem disturbances (Potter et al., 2003b).

Our analysis requires data transformations to detect anomalies. The first step in this analysis of interannual variability was the conversion of all time series to monthly  $Z$ -score values, which can be used to specify the relative statistical location of each monthly value within the 17-yr population distribution (e.g., all Januarys are adjusted with respect to the long-term mean January value). The numerical  $Z$  score indicates the distance from the long-term monthly mean as the number of standard deviations above or below the mean. The main difference between the  $t$  statistic and the  $Z$  score is that the  $Z$  score uses a monthly sample standard deviation, whereas the  $t$  score uses population standard deviation, which is usually unknown.

While our NASA–CASA model results show several consecutive multiyear periods during which the magnitudes of continental NA sinks for  $\text{CO}_2$  were fairly constant, the predicted spatial pattern of these sink fluxes was actually quite variable from one year to the next. Areas showing the highest interannual variability on NEP fluxes were defined according to the number of anomalously low (LO) or anomalously high (HI) monthly events detected in the 17-yr time series. We used an anomalous event threshold value of 1.7 standard deviations (SDs) LO or HI relative to the long-term (1982–98) NEP monthly mean value. In the use of a one-tailed (LO or HI) statistical  $t$  test, rejection of the null hypothesis means that there is no difference between the 17-yr average for the monthly NEP level and an anomalous monthly event. In separate one-tailed tests for LO and HI events, an  $\text{SD} > 1.7$  represents the 95% confidence level for outliers in the population (Stockburger, 1998). Additionally, a threshold value of greater than three anomalous NEP-LO or NEP-HI monthly events, representing anomaly sums just inside the 99th percentile, was used to identify the areas of high interest for interannual variability, which also ensures that at all locations identified there would have been, on average, at least one anomalous monthly event detected every 5 years in the time series.

An example NEP time series for a forest site (DeFries and Townshend, 1994) in southeastern Canada (Figure 3) illustrates a location where we can detect more than twice the number of anomalously HI versus LO monthly events. The strong seasonal signal in “raw” NEP predictions directly from the NASA–CASA model dominates the time series pattern, which is typical for the Northern Hemisphere carbon cycle. The  $Z$ -score-transformed time series is shown below the raw NEP panel. Although there is not a readily evident upward or downward trend in the  $Z$ -score time series, this selected location with its high number of anomalous NEP-HI events, illustrates a forest area that has been a net sink for carbon over the past two decades (Potter et al., 2003a).

For our regional analysis, association patterns are reported with respect to the U.S. Department of Agriculture’s Major Land Resource Areas (MLRA; U.S. Department of Agriculture, 1981). High interannual variability in NEP fluxes can be readily identified at locations across the continent, which approach the maximum of 20 cumulative NEP-LO or NEP-HI monthly events in the time series (Figure 4). According to the distribution of NEP-LO events (Figure 4a), the areas

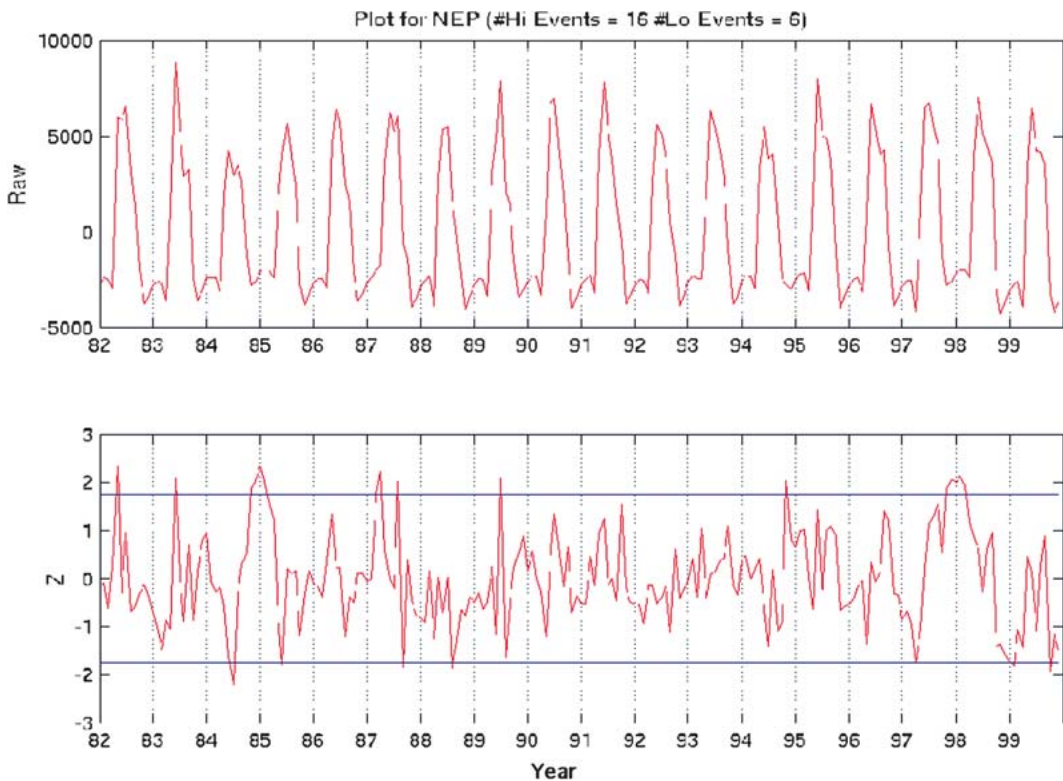


**Figure 3. Time series example (1982–99) of (top) NEP raw values and (bottom) Z-score (units = SD) line plot for a temperate forest ecosystem location in southern Quebec (47°N, 67°W). Units of raw NEP are  $10^2 \text{ g C m}^{-2} \text{ mo}^{-1}$ . Horizontal lines in the bottom panel mark the 1.7-SD threshold level for defining anomalously LO and HI monthly events.**

of highest variability are detected along the extreme northern vegetated zones of Canada and Alaska, the southern United States and Mexico, and the central-western U.S. Great Plains. According to the distribution of NEP-HI events (Figure 4b), the areas of highest variability are detected along the eastern and western coastal areas of the United States and Canada, the U.S. central farming and forest region, the northern Rocky Mountains, and interior Alaska. There is minimal overlap between the areas of highest cumulative NEP-LO versus NEP-HI monthly events in these two figures.

#### 4. Associations with climate events

Association analysis can offer further insights into the types of dependencies that exist among variables within a large dataset (Agrawal and Srikant, 1994). Anomalously LO or anomalously HI monthly events for the main NASA–CASA model time series inputs of TEMP, PREC, SOLAR, and FPAR can be mapped in association with LO or HI monthly events for predicted NEP. As in the case of

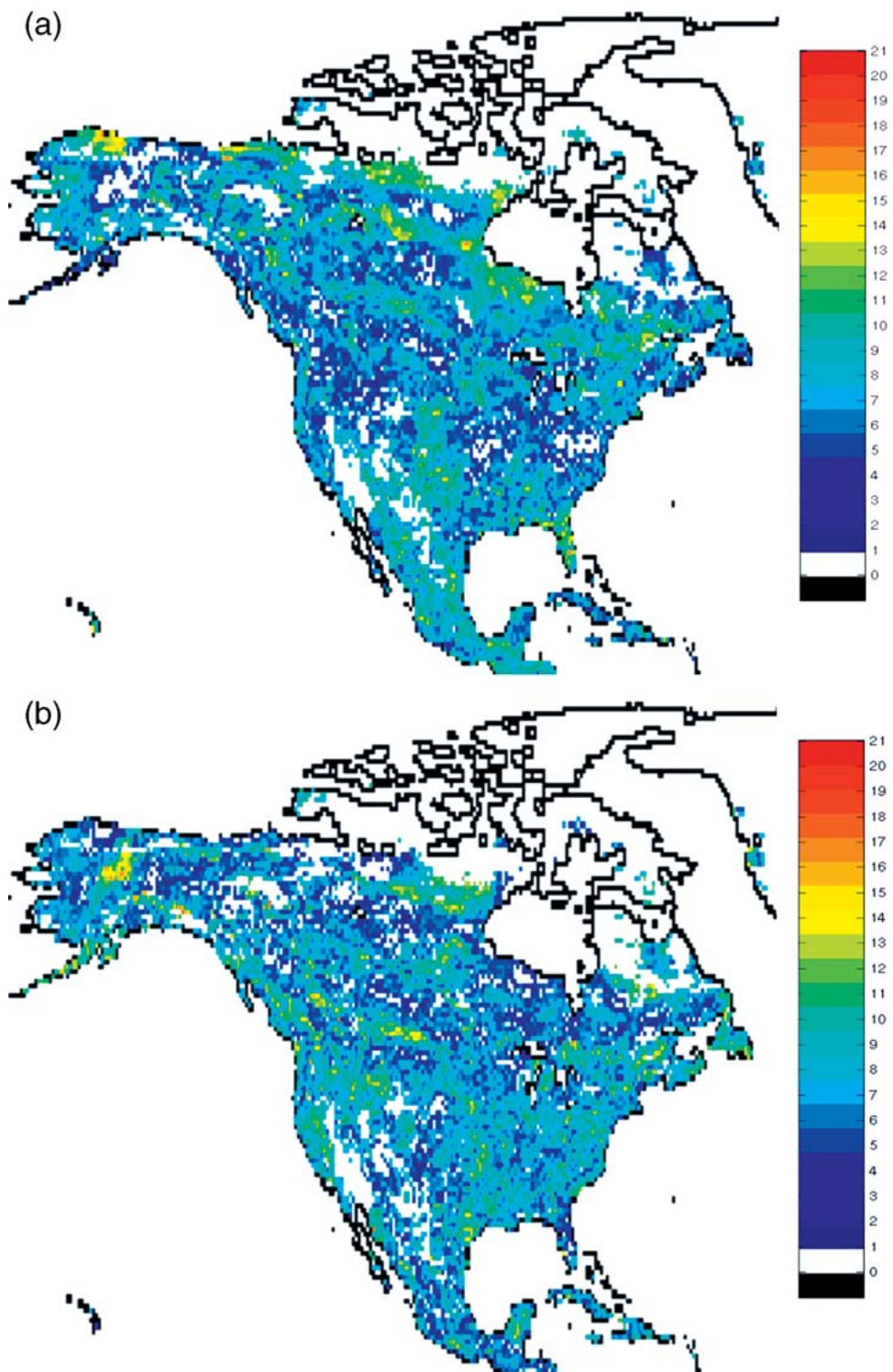


Figure 4. Location of NEP monthly anomalies in the 17-yr time series (1982–98) for (a) NEP-LO anomalies and (b) NEP-HI anomalies. Color bar shows number of LO or HI anomalous events at each pixel location.

NEP, we used an anomalous event threshold value of 1.7 SD or greater from the long-term (1982–98) climatic monthly mean value.

It is important to note that, because the NASA–CASA model has numerous nonlinear functions that are used to transform the input variables of TEMP, PREC, SOLAR, and FPAR into predicted ecosystem NEP fluxes, a large fraction of anomalously LO or HI monthly events for NEP detected in Figure 4 may have no consistent associations with the four input variables at the selected threshold value. This is not to imply that one input variable or another is not a dominant control over NEP fluxes simply because we do not report it as such in the association counts below. To the contrary, many nonlinear dependencies between model inputs and NEP predictions may fall below our threshold values of 1.7 SD; hence, we can compare the association counts among the four input variables with NEP anomalies only in a relative sense, rather than in an effort to explain all or most of the continent-wide NEP-LO and NEP-HI monthly events depicted in Figure 4. Association counts presented below should be considered representative samples of the strongest dependencies between NEP and at least one of the four input variables, rather than an exhaustive analysis of controls on NEP at every land location in Figure 4.

In the association counts of NEP with anomalous FPAR or SOLAR monthly events, we considered only two possible cases, LO with LO and HI with HI, because these two model inputs operate solely in NPP model calculations in a near-linear fashion to alter NEP estimates. The near-linear form of this relationship derives from the empirical calibration in our original CASA model for NPP (Potter et al., 1993). This means that FPAR-LO or SOLAR-LO can decrease NPP (but not soil  $R_h$ ) and hence potentially result in a NEP-LO monthly event (but not in an NEP-HI monthly event). The reverse effect on NPP-HI events (but not on soil  $R_h$ ) can result from FPAR-HI or SOLAR-HI monthly events. In the association counts of NEP with anomalous TEMP or PREC monthly events, we instead considered all four possible cases, LO with LO, LO with HI, HI with LO, and HI with HI, because these two model inputs operate in both NPP and soil  $R_h$  model calculations to alter NEP estimates.

The most readily detectable association between model input events and NEP monthly events for North America was with anomalous FPAR (LO and HI combined) monthly events (Table 1), followed in decreasing order by SOLAR, PREC, and TEMP monthly events. Using the same threshold value of greater than three anomalous monthly events with  $SD > 1.7$  in the 17-yr time series to identify pixels of interest, FPAR monthly anomalies were detected to co-occur with NEP monthly anomalies at about 9% of all the areas shown in Figure 4, whereas SOLAR monthly anomalies were detected to co-occur with NEP monthly anomalies at about 5% of all the pixel areas shown in Figure 4.

FPAR-LO monthly anomalies were detected to co-occur with NEP-LO monthly anomalies mainly in central Mexico, the western U.S. Great Plains, and the Rocky Mountain range, whereas FPAR-HI monthly anomalies were detected to co-occur with NEP-HI monthly anomalies mainly in northeastern Mexico, the western U.S. Great Plains, and eastern Canada (Figure 5a). These spatial patterns suggest that NEP is most heavily influenced by FPAR anomalies in areas that are semiarid and/

**Table 1. Counts of 0.5° pixels in NA for co-occurrence of model input events with NEP monthly anomalous events.**

	NEP-LO Total 8718	NEP-HI Total 8509
MODEL INPUTS		
TEMP-LO	111	54
TEMP-HI	79	21
PREC-LO	10	18
PREC-HI	634	102
SOLAR-LO	487	—
SOLAR-HI	—	342
FPAR-LO	935	—
FPAR-HI	—	647

or frequently cropped, both of which can respond fairly rapidly to variable rainfall patterns.

SOLAR-LO monthly anomalies were detected to co-occur with NEP-LO monthly anomalies mainly in the Rocky Mountain range and into interior Alaska, whereas SOLAR-HI monthly anomalies were detected to co-occur with NEP-HI monthly anomalies mainly along Canada's southern coastal zones (Atlantic and Pacific), the U.S. Pacific Northwest, and coastal Alaska (Figure 5b). These spatial patterns suggest that NEP is most heavily influenced by SOLAR anomalies in areas that are high in elevation or in close proximity to a coastal zone, both of which are impacted by frequent cloud cover.

Another notable association was observed for PREC-HI monthly anomalies that were detected to co-occur with NEP-LO monthly anomalies (Table 1) for about 7% of all the areas shown in Figure 4. These pixels are aggregated mainly in the combined areas of northern Mexico, the southwestern U.S. rangelands, and the central-western U.S. Great Plains. This association pattern is more difficult to explain than are patterns of FPAR and SOLAR anomalies with NEP anomalies (Figure 5). One possible explanation is that PREC-HI monthly anomalies in these areas are associated with seasons of high accumulated biomass fuel that can burn rapidly when ignited by lightning strikes. A major wildfire at these locations would depress NPP and result in a NEP-LO monthly anomaly.

## 5. Conclusions

Our NASA–CASA model results reveal important patterns of geographic variability in NEP within major continental areas of the terrestrial biosphere. A unique advantage of combining ecosystem modeling with global satellite sensor drivers for vegetation cover properties is to enhance the spatial resolution of sink patterns for CO<sub>2</sub> in the terrestrial biosphere. On the temporal scale, this AVHRR dataset used to generate FPAR input to the NASA–CASA model now extends for nearly 20 yr of global monthly imagery, which permits model evaluations within the context of other global long-term datasets for climate and atmospheric CO<sub>2</sub> levels. We have begun to identify numerous relatively small-scale patterns

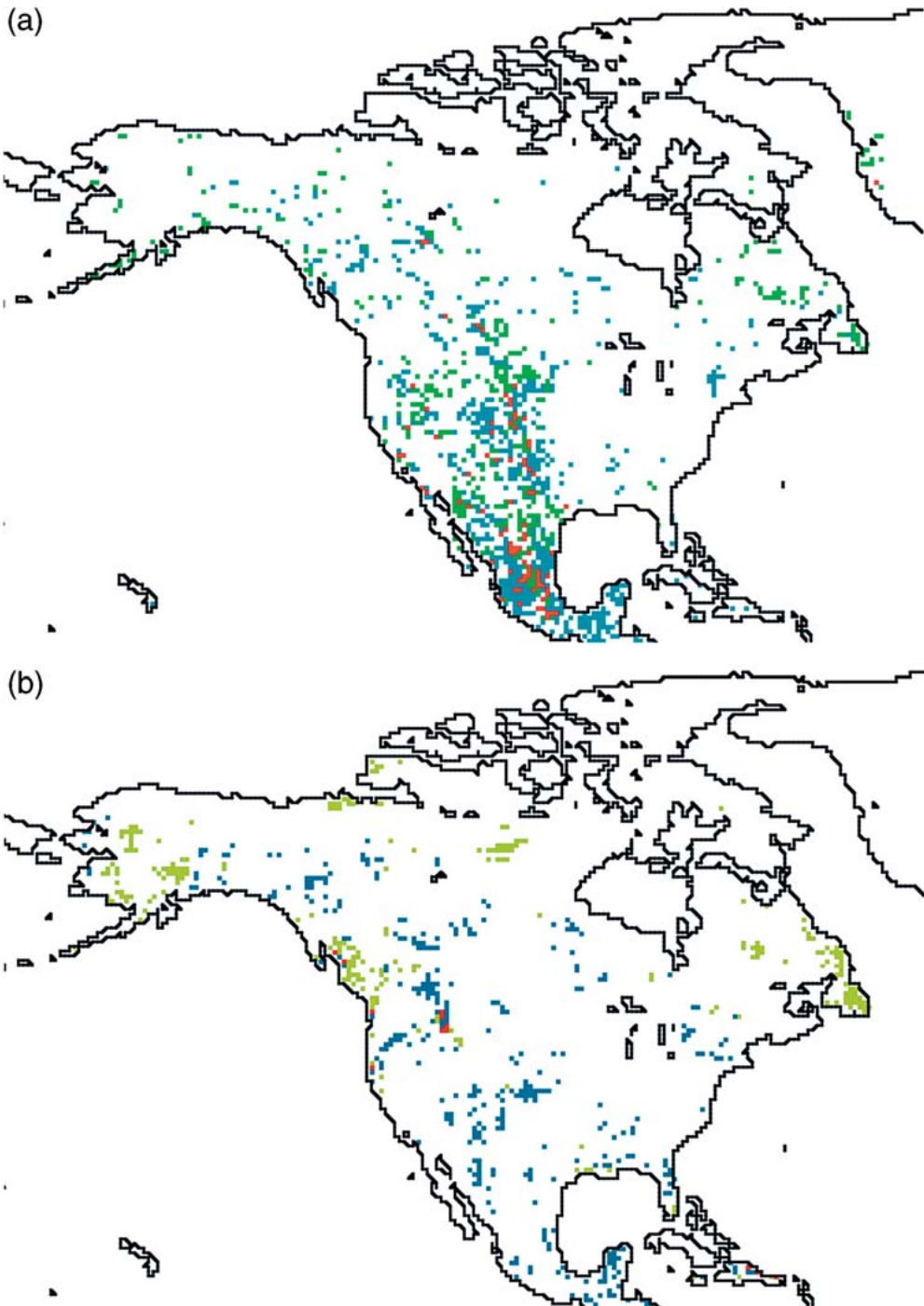


Figure 5. Collocation of NEP monthly anomalies in the 17-yr time series (1982–98) with (a) FPAR monthly anomalies and (b) SOLAR monthly anomalies. Each colored pixel meets a threshold value of greater than three co-occurring events during the entire time series. Green pixels are LO–LO event associations, blue pixels are HI–HI event associations, and red pixels are both LO–LO and HI–HI event associations.

throughout the world where terrestrial carbon fluxes may vary between net annual sources and sinks from one year to the next. Predictions of NEP for these areas of high interannual variability will require further validation of carbon model estimates, with focus on both flux algorithm mechanisms and potential scaling errors to the regional level.

**Acknowledgments.** This work was supported by grants from NASA programs in Intelligent Systems and Intelligent Data Understanding, and the NASA Earth Observing System (EOS) Interdisciplinary Science Program. We thank Joseph Coughlan of NASA Ames Research Center and two anonymous reviewers for helpful comments on an earlier version of the manuscript.

## References

- Agrawal, R., and R. Srikant, 1994: Fast algorithms for mining association rules in large databases, paper presented at 20th International Conference on Very Large Data Bases (VLDB'94), Santiago, Chile, 12–15 September 1994.
- Amthor, J. S., et al., 2001: Boreal forest CO<sub>2</sub> exchange and evapotranspiration predicted by nine ecosystem process models: Inter-model comparisons and relations to field measurements. *J. Geophys. Res.*, **106**, 33,623–33,648.
- Behrenfeld, M. J., et al., 2001: Biospheric primary production during an ENSO transition. *Science*, **291**, 2594–2597.
- Bolin, B., Ed., 1981: Carbon Cycle Modeling. *SCOPE Report No. 16*, John Wiley.
- DeFries, R., and J. Townshend, 1994: NDVI-derived land cover classification at global scales. *Intl. J. Remote Sens.*, **15**, 3567–3586.
- FAO, 1995: Digital Soil Map of the World and Derived Soil Properties (Version 3.5). FAO, Rome, Italy.
- Goetz, S. J., and S. D. Prince, 1998: Variability in light utilization and net primary production in boreal forest stands. *Can. J. For. Res.*, **28**, 375–389.
- Hicke, J. A., G. P. Asner, J. T. Randerson, C. J. Tucker, S. O. Los, R. Birdsey, J. C. Jenkins, C. B. Field, and E. A. Holland, 2002: Satellite-derived increases in net primary productivity across North America, 1982–1998. *Geophys. Res. Lett.*, **29**, 1427, doi:10.1029/2001GL013578.
- Kindermann, J., G. Würth, and G. H. Kohlmaier, 1996: Interannual variation of carbon exchange fluxes in terrestrial ecosystems. *Global Biogeochem. Cycles*, **10**, 737–755.
- Knyazikhin, Y., J. V. Martonchik, R. B. Myneni, D. J. Diner, and S. W. Running, 1998: Synergistic algorithm for estimating vegetation canopy leaf area index and fraction of absorbed photosynthetically active radiation from MODIS and MISR data. *J. Geophys. Res.*, **103**, 32,257–32,276.
- Maisongrand, P., A. Ruimy, G. Dedieu, and B. Saugier, 1995: Monitoring seasonal and interannual variations of gross primary productivity, net primary productivity, and net ecosystem productivity using a diagnostic model and remotely sensed data. *Tellus*, **47B**, 178–190.
- Malmström, C. M., M. V. Thompson, G. P. Juday, S. O. Los, J. T. Randerson, and C. B. Field, 1997: Interannual variation in global scale net primary production: Testing model estimates. *Global Biogeochem. Cycles*, **11**, 367–392.
- McGuire, A. D., et al., 2001: Carbon balance of the terrestrial biosphere in the twentieth century: Analyses of CO<sub>2</sub>, climate and land-use effects with four process-based ecosystem models. *Global Biogeochem. Cycles*, **15**, 183–206.

- Nemani, R. R., and S.W. Running, 1989: Testing a theoretical climate–soil–leaf area hydrologic equilibrium of forests using satellite data and ecosystem simulation. *Agric. For. Meteorol.*, **44**, 245–260.
- Nemani, R., M. White, P. Thornton, K. Nishida, S. Reddy, J. Jenkins, and S. Running, 2002: Recent trends in hydrologic balance have enhanced the terrestrial carbon sink in the United States. *Geophys. Res. Lett.*, **29**, 1468, doi:10.1029/2002GL014867.
- New, M., M. Hulme, and P. Jones, 2000: Representing twentieth century space–time climate variability. Part II: Development of 1901–1996 monthly grids of terrestrial surface climate. *J. Clim.*, **13**, 2217–2238.
- Potter, C. S., 1999: Terrestrial biomass and the effects of deforestation on the global carbon cycle. *BioScience*, **49**, 769–778.
- Potter, C. S., J. T. Randerson, C. B. Field, P. A. Matson, P. M. Vitousek, H. A. Mooney, and S. A. Klooster, 1993: Terrestrial ecosystem production: A process model based on global satellite and surface data. *Global Biogeochem. Cycles*, **7**, 811–841.
- Potter, C. S., S. A. Klooster, and V. Brooks, 1999: Interannual variability in terrestrial net primary production: Exploration of trends and controls on regional to global scales. *Ecosystems*, **2**, 36–48.
- Potter, C. S., J. Bubier, P. Crill, and P. LaFleur, 2001: Ecosystem modeling of methane and carbon dioxide fluxes for boreal forest sites. *Can. J. For. Res.*, **31**, 208–223.
- Potter, C. S., S. A. Klooster, R. B. Myneni, V. Genovese, P.-N. Tan, and V. Kumar, 2003a: Continental scale comparisons of terrestrial carbon sinks estimated from satellite data and ecosystem modeling 1982–1998. *Global Planet. Change*, **30**, 201–213.
- Potter, C., P. Tan, M. Steinbach, S. Klooster, V. Kumar, R. Myneni, and V. Genovese, 2003b: Major disturbance events in terrestrial ecosystems detected using global satellite data sets. *Global Change Biol.*, **9**(7), 1005–1021.
- Running, S. W., and R. R. Nemani, 1998: Relating seasonal patterns of the AVHRR vegetation index to simulated photosynthesis and transpiration of forests in different climates. *Remote Sens. Environ.*, **24**, 347–367.
- Schimel, D., et al., 2001: Recent patterns and mechanisms of carbon exchange by terrestrial ecosystems. *Nature*, **414**, 169–172.
- Sellers, P. J., C. J. Tucker, G. J. Collatz, S. O. Los, C. O. Justice, D. A. Dazlich, and D. A. Randall, 1994: A global 1×1 NDVI data set for climate studies. Part 2: The generation of global fields of terrestrial biophysical parameters from the NDVI. *Intl. J. Remote Sens.*, **15**, 3519–3545.
- Stockburger, D. W., 1998: *Introductory Statistics: Concepts, Models, and Applications*. Version 1.0. [Available online at <http://www.psychstat.smsu.edu/sbk00.htm>.]
- U.S. Department of Agriculture, 1981: U.S.D.A. Soil Conservation Service, Land Resource Regions and Major Land Resource Areas of the United States. USDA Agricultural Handbook No. 296, 156 pp.